Diabetologia (2010) 53:1986–1997
DOI 10.1007/s00125-010-1788-7

ARTICLE

Naturally occurring R225W mutation of the gene encoding AMP-activated protein kinase (AMPK)γ_3 results in increased oxidative capacity and glucose uptake in human primary myotubes

S. A. Crawford · S. R. Costford · C. Aguer · S. C. Thomas · R. A. deKemp · J. N. DaSilva · D. Lafontaine · M. Kendall · R. Dent · R. S. B. Beanlands · R. McPherson · M.-E. Harper

Received: 31 October 2009 / Accepted: 12 April 2010 / Published online: 15 May 2010

Abstract
Aims/hypothesis AMP-activated protein kinase (AMPK) has a broad role in the regulation of glucose and lipid metabolism making it a promising target in the treatment of type 2 diabetes mellitus. We therefore sought to characterise for the first time the effects of chronic AMPK activation on skeletal muscle carbohydrate metabolism in carriers of the rare gain-of-function mutation of the gene encoding AMPKγ_3 subunit, *PRKAG3* R225W.

Methods Aspects of fuel metabolism were studied in vitro in myocytes isolated from vastus lateralis of *PRKAG3* R225W carriers and matched control participants. In vivo, muscular strength and fatigue were evaluated by isokinetic dynamometer and surface electromyography, respectively. Glucose uptake in exercising quadriceps was determined using [^{18}F]fluorodeoxyglucose and positron emission tomography.

Results Myotubes from *PRKAG3* R225W carriers had threefold higher mitochondrial content ($p<0.01$) and oxidative capacity, higher leak-dependent respiration (1.6-fold, $p<0.05$), higher basal glucose uptake (twofold, $p<0.01$) and higher glycogen synthesis rates (twofold, $p<0.05$) than control myotubes. They also had higher levels of intracellular glycogen ($p<0.01$) and a trend for lower intramuscular triacylglycerol stores. R225W carriers showed remarkable resistance to muscular fatigue and a trend for increased glucose uptake in exercising muscle in vivo.

Conclusions/interpretation Through the enhancement of skeletal muscle glucose uptake and increased mitochondrial content, the R225W mutation may significantly enhance exercise performance. These findings are also consistent with the hypothesis that the γ_3 subunit of AMPK is a promising tissue-specific target for the treatment of type 2 diabetes mellitus, a condition in which glucose uptake and mitochondrial function are impaired.

Keywords AMP-activated protein kinase · Glucose uptake · Mitochondria · Oxidative capacity · Skeletal muscle · Type 2 diabetes mellitus

Electronic supplementary material The online version of this article (doi:10.1007/s00125-010-1788-7) contains supplementary material, which is available to authorised users.

S. A. Crawford · S. R. Costford · C. Aguer · M.-E. Harper (✉)
Department of Biochemistry, Microbiology and Immunology,
Faculty of Medicine, University of Ottawa,
451 Smyth Road,
Ottawa, ON, Canada K1H 8M5
e-mail: mharper@uottawa.ca

R. A. deKemp · J. N. DaSilva · R. S. B. Beanlands · R. McPherson
University of Ottawa Heart Institute,
Ottawa, ON, Canada

D. Lafontaine · M. Kendall
School of Human Kinetics, University of Ottawa,
Ottawa, ON, Canada

S. C. Thomas
Human Physiology, Pennington Biomedical Research Center,
Baton Rouge, LA, USA

R. Dent
Ottawa Hospital Weight Management Clinic,
Ottawa, ON, Canada

Abbreviations

AICAR	Aminoimidazole carboxamide ribonucleotide
AMPK	AMP-activated protein kinase
FCCP	Carbonyl cyanide-*p*-trifluoromethoxyphenylhydrazone
FDG	[^{18}F]Fluorodeoxyglucose
IMTG	Intramuscular triacylglycerol
MnSOD	Manganese superoxide dismutase
PET	Positron emission tomography
PGC-1α	Peroxisome proliferator-activated receptor γ coactivator 1α
SUV	Standard uptake value
TCA	Tricarboxylic acid

Introduction

AMP-activated protein kinase (AMPK) is a heterotrimeric enzyme that can form 12 distinct complexes, each comprising an α catalytic subunit (α_1 or α_2), as well as a β and a γ regulatory subunit (β_1, β_2; γ_1, γ_2 or γ_3), as reviewed by Hardie and by Steinberg et al [1, 2] respectively. All AMPK subunits can be detected to some extent in skeletal muscle; however, it is thought that only three of the possible 12 heterotrimeric complexes are formed there: $\alpha_1/\beta_2/\gamma_1$, $\alpha_2/\beta_2/\gamma_1$ and $\alpha_2/\beta_2/\gamma_3$ [3]. The γ_3 subunit is exclusively produced in skeletal muscle and appears to be most highly abundant in fast-twitch glycolytic (type IIb) muscle fibres [4, 5].

The AMP-dependent activation of AMPK in skeletal muscle enables it to act as a major energy sensor within the cell by detecting intracellular levels of ATP and AMP through specific binding sites on the γ regulatory subunit [6–8]. AMPK may also be regulated through the glycogen-binding domain on the β subunit by the content and structure of intracellular glycogen [9]. When stimulated, AMPK acts to restore cellular energy balance by stimulating ATP-producing pathways (glucose uptake, fatty acid oxidation and mitochondrial biogenesis) [10–13] and inhibiting ATP-consuming pathways (fatty acid synthesis, glycogen synthesis and protein synthesis) [14–17].

The rare but naturally occurring R225W mutation in the gene (*PRKAG3*) encoding the AMPKγ_3 subunit in humans was previously identified by our laboratory as a gain-of-function mutation that results in a doubling of basal and AMP-stimulated AMPK activity [18]. In addition to increased AMPK activity, participants carrying the R225W mutation were shown to have ~90% higher glycogen content and ~30% lower intramuscular triacylglycerol (IMTG) content in the vastus lateralis muscle [18]. This mutation is homologous to the *PRKAG3* R225Q mutation in *RN*$^-$ Hampshire pigs, which causes high muscle glycogen content [19], as well as to the *PRKAG2* R302Q mutation in humans, which is associated with Wolff–Parkinson–White syndrome [20–22]. Several mouse models have also been developed either to overproduce the AMPKγ_3 subunit or to express the gain-of-function *Prkag3* R225Q mutation [23, 24]. Recently, Garcia-Roves et al. [24] demonstrated that while the overproduction or ablation of the AMPKγ_3 subunit in mice did not alter mitochondrial biogenesis, expression of *PRKAG3* R225Q (similar to the R225W mutation studied herein) resulted in enhanced mitochondrial biogenesis.

The *PRKAG3* R225Q, *PRKAG3* R225W and *PRKAG2* R302Q mutations are associated with excess glycogen in skeletal muscle (*PRKAG3*) or in heart (*PRKAG2* R302Q) [18–20]. Although AMPK inhibits glycogen synthesis through phosphorylation of glycogen synthase, the allosteric activation of glycogen synthase by glucose 6-phosphate can overcome the inhibitory effects of glycogen synthase phosphorylation [25, 26]. Studies have demonstrated that AMPK activation in the heart and skeletal muscle enhances GLUT4 transport to the plasma membrane [27, 28] and that loss of the AMPK α_2, β_2 or γ_3 subunits abolishes aminoimidazole carboxamide ribonucleotide (AICAR)-stimulated glucose uptake [23, 29]. While the mechanisms underlying the AMPK-mediated increases in glucose uptake have not been fully elucidated, AMPK has been shown to phosphorylate and activate TBC1 domain family, member 4 (TBC1D4) and the IRS-1, both of which stimulate GLUT4 translocation [30, 31]. Additionally, chronic AMPK activation in Sprague–Dawley rats through treatment with AICAR increases skeletal muscle levels of GLUT4 and hexokinase [32]. The present study characterises for the first time the effects of chronic AMPK activation on skeletal muscle carbohydrate metabolism in carriers of the rare gain-of-function mutation of the gene encoding the-AMPKγ_3 subunit, *PRKAG3* R225W.

Methods

Participants Two probands carrying the *PRKAG3* R225W mutation were initially identified through the Ottawa Hospital Weight Management Clinic [18]. Four R225W carriers were recruited for this study and matched for age, sex, BMI and physical activity (International Physical Activity Questionnaire) to control participants. All four participants underwent in vivo positron emission tomography (PET) imaging and isokinetic dynamometer strength determinations; one of the four participants did not consent to a skeletal muscle biopsy and was therefore not included in the cellular studies. The protocol for this study was approved by the Research Ethics Board of the Ottawa

Hospital and the University of Ottawa Heart Institute. Written informed consent was obtained from all participants.

Muscular strength and fatigue determination Participants were screened for physical activity readiness by Physical Activity Readiness Questionnaire. Following a 12 h overnight fast, participants underwent testing to determine the maximal force output of the quadriceps in their dominant leg using an isokinetic dynamometer (Kin Com; Isokinetic International, Harrison, TN, USA). Participants performed a series of three to five constant velocity (60°/s) concentric and eccentric contractions for determination of maximal force output. The rate of muscular fatigue in the vastus lateralis, vastus medialis and rectus femoris muscles was evaluated by electromyography. The change in the mean frequency of contraction was monitored over the course of a 60 s isometric contraction of the quadriceps at 80% of the participant's maximal eccentric force. Data collection and processing were performed using an electromyography unit (Bortec, Calgary, AB, Canada) (sampling rate 1,000 Hz) connected to a movement and behaviour analysis system (SIMI, Unterschleissheim, Germany).

Exercise intervention and [^{18}F]fluorodeoxyglucose PET Participants refrained from physical activity for 48 h and underwent a 12 h overnight fast prior to the exercise intervention. Immediately before the initiation of exercise, a baseline blood sample was taken for determination of serum NEFA, cortisol, insulin, lactate and glucose concentrations. Keeping their non-dominant leg in the resting position, participants performed leg extensions with the dominant leg for 30 min, bearing a load equivalent to 11% of their maximal concentric force output as determined during strength testing. The leg extension consisted of a 1 s concentric phase and a 2 s eccentric phase. [^{18}F]Fluorodeoxyglucose (FDG) is retained within the cell and can be quantified using PET [33]. FDG (5 MBq/kg) was injected 10 min post exercise initiation and exercise proceeded for an additional 20 min [34, 35]. Blood samples were taken for metabolite analysis immediately prior to FDG injection, and at 20 and 60 min post-injection. After 30 min of exercise, participants underwent a computed tomography scan followed by a 20 min PET scan in 3D mode (Discovery Rx PET/VCT; GE Healthcare, Milwaukee, WI, USA). FDG PET images were reconstructed using a 3D iterative algorithm (ordered subset expectation maximisation 21 subsets, two iterations) with a 4 mm Hann post-reconstruction filter. Images were quantified in terms of the standardised uptake value (SUV), with SUV=pixel value (Bq/ml)×body weight (kg)/injected activity (kBq). A volume of interest was defined over the quadriceps muscle in the exercised leg using a threshold value of SUV>1.0 (Hybrid Viewer; HERMES Medical Solution, Stockholm, Sweden). The mean and integral SUV was measured within the volume of interest.

Skeletal muscle biopsies Participants refrained from physical activity for 3 days and fasted for 12 h prior to the biopsy. After local anaesthesia, biopsies of the vastus lateralis were obtained using a 5 mm Bergstrom needle (Opitek International, Glostrup, Denmark) as previously described [18].

Cell culture Freshly biopsied vastus lateralis was minced, subjected to 30 min trypsin digestion and plated in Ham's F-10 medium, supplemented with 15% FBS (vol./vol.), 0.5 mg/ml BSA, 1 μmol/l dexamethazone, 10 ng/ml EGF, 0.5 mg/ml fetuin and 25 pmol/l insulin. Muscle satellite cells were isolated as described previously [18] using anti-5.1H11 antibody (Developmental Studies Hybridoma Bank) [36]. Prior to experimentation, isolated myoblasts were grown to ~80% confluence prior to differentiation for 7 days in 5.5 mmol/l glucose DMEM (with 25 pmol/l insulin, 2% horse serum [vol./vol.], 1% antibiotic–antimycotic [vol./vol.] and 2.5 mg/ml gentamicin).

Mitochondrial enzyme activities Mitochondria were isolated from myotubes using a mitochondrial isolation kit (MITOISO2; Sigma, St Louis, MO, USA). Mitochondrial and total cellular protein were determined by bicinchoninic acid assay. Cytochrome *c* oxidase activity was assayed in intact mitochondria using a kit (CYTOCOX1; Sigma). Citrate synthase activity was determined in lysed mitochondria using a kit (CS0720; Sigma).

Oxygen consumption Oxygen consumption was measured in myotubes using an analyser (Extracellular Flux Analyser; Seahorse Bioscience, North Billerica, MA, USA). Myoblasts were seeded 50,000 per well in specialised 24-well plates (Seahorse Bioscience). Myotubes were incubated for 1 h at 37°C in DMEM (5030; Sigma) supplemented with 5.5 mmol/l D-glucose and 0.584 g/l L-glutamine prior to analysis. Baseline oxygen consumption was measured four times for 3 min at 7 min intervals. Carbonyl cyanide-*p*-trifluoromethoxyphenylhydrazone (FCCP) (1 μmol/l) or oligomycin (500 ng/ml) was then injected into each well and mixed for 10 min prior to measurement.

Intramuscular triacylglycerol content IMTG content was determined in myotubes treated with or without 2 mmol/l AICAR for 2 h. Myotubes were resuspended in 25 mmol/l Tris–HCl pH 7.5 with 1 mmol/l EDTA. Lipids were extracted via chloroform–methanol (2:1), dried under N_2 gas and dissolved in 2-propanol. IMTG concentration was determined using an assay (L-Type TG H; Wako Chemicals, Richmond, VA, USA) and normalised to protein content.

Fatty acid oxidation assay In a 12-well plate, myoblasts were grown to ~80% confluency in low glucose DMEM supplemented with 10% FBS (vol./vol.), 0.5 mg/ml BSA, 1 μmol/l dexamethazone, 10 ng/ml human EGF, 0.5 mg/ml fetuin, 50 μg/ml gentamicin and 0.05 μg/ml fungizone. They were then differentiated for 5 days in α-MEM media supplemented with 2% FBS (vol./vol.), 2% PenStrep (vol./vol.) and 0.5 mg/ml fetuin. Cells were exposed for 3 h to incubation media containing 100 μmol/l cold palmitate, 37 kBq/ml [1-^{14}C]palmitate (Perkin Elmer, Waltham, MA, USA), 0.25% fatty acid-free BSA (wt/vol.), 1 mmol/l carnitine and 12.5 mmol/l HEPES. Incubation medium was then transferred to a 24 dual-well Teflon trapping plate [37] and the reaction terminated by adding 70% perchloric acid (wt/vol.). During 1 h incubation at 25°C, $^{14}CO_2$ was trapped in 1 mol/l sodium hydroxide and quantified by liquid scintillation counting. Incubation medium was left overnight at 4°C and centrifuged at 15,000 *g* for 5 min, after which the ^{14}C-labelled acid soluble metabolites were quantified.

Fatty acid uptake Myoblasts were grown as described and differentiated for 6 days. Fatty acid uptake rates were determined as previously described [38]. Cells were incubated with or without 100 nmol/l insulin for 20 min and then for 4 min in FBS-free medium containing 7.4 kBq/ml [1-^{14}C]palmitic acid (Perkin Elmer) and 20 μmol/l cold palmitate conjugated to fatty acid-free BSA. Cells were then washed with ice-cold PBS and collected with 0.1 mol/l NaOH.

Glycogen content Myotubes were suspended in PBM buffer (20 mmol/l KH_2PO_4, 10 μmol/l $CaCl_2$, 1 mmol/l $MgCl_2$, pH 6.1) and lysed by freeze–thaw. Samples were boiled for 20 min in 30% KOH (wt/vol.) saturated with anhydrous Na_2SO_4. Glycogen was precipitated with 95% ethanol (vol./vol.), dissolved in double distilled H_2O and incubated for 20 min with 0.2% anthrone (wt/vol.) in H_2SO_4 at 100°C. Glycogen concentration was determined spectrophotometrically relative to an oyster glycogen standard curve and normalised to protein content.

Glucose uptake Glucose uptake was assayed as described previously [39]. Myotubes were washed with uptake buffer (136 mmol/l NaCl, 4.7 mmol/l KCl, 1.25 mmol/l $MgSO_4 \cdot 7H_2O$, 1.2 mmol/l $CaCl \cdot 2H_2O$, 20 mmol/l HEPES; pH 7.4) and incubated at 37°C for 20 min with or without 100 nmol/l insulin. Cells were exposed to 18.5 kBq/ml 2-deoxy[^{3}H]glucose and 100 μmol/l cold 2-deoxy-glucose for 10 min, then washed and collected.

Glycogen synthesis Glycogen synthesis was assayed as described previously [40]. Myotubes were glucose/serum-starved for 1.5 h, incubated for 3 h in DMEM containing 5.5 mmol/l glucose and 18.5 kBq/ml 2-deoxy[^{3}H]glucose with or without 100 nmol/l insulin, and then washed and collected. Lysates were incubated for 20 min at 100°C in the presence of 6.3 μg/μl oyster glycogen. Glycogen was precipitated in ethanol, washed and then dissolved in double distilled H_2O.

RNA extraction and quantitative RT-PCR RNA was extracted from myotubes with Trizol and flash-frozen. RNA was column-purified using a kit (RNeasy Fibrous Mini Kit; Qiagen, Mississagua, ON, Canada). Primers and probes were designed for *PGC-1α* (also known as *PPARGC1A*), *mTFA* (also known as *TFAM*) and *NRF1* using Primer Express 2.1 (Applied Biosystems) (Electronic supplementary material [ESM] Table 1). The concentration of target mRNAs was determined by quantitative RT PCR using Taqman primers and fluorescent probes as detection system. The quantitative RT-PCR was performed on a device (ABI PRISM 7900; Applied Biosystems, Foster City, CA, USA) using the following variables: one cycle of 48°C for 30 min, then 95°C for 10 min, followed by 40 cycles at 95°C for 15 s and at 60°C for 1 min. All expression data were normalised to the housekeeping gene *RPLP0*.

Western blotting Electrophoresis of cell lysates was carried out on 10% polyacrylamide gel (wt/vol.) and proteins were transferred to a nitrocellulose membrane. Primary antibodies were: manganese superoxide dismutase (MnSOD) (sc-30080; Santa-Cruz, Santa Cruz, CA, USA), peroxisome proliferator-activated receptor γ coactivator 1α (PGC-1α) (sc-13067; Santa-Cruz), cytochrome *c* oxidase (MS404; MitoSciences, Eugene, OR, USA), P-Akt (Ser473 #9271; Cell Signaling, Beverly, MA, USA), Akt (9272; Cell Signaling) and β-actin (4967 L; Cell Signaling). Secondary antibodies were: goat anti-rabbit horseradish peroxidase and goat anti-mouse horseradish peroxidase (sc-2030 and sc-2031, respectively; Santa Cruz). Visualisation was achieved using a chemiluminescence kit (ECL; Amersham Pharmacia, Pittsburgh, PA, USA).

Statistical methods A Student's *t* test or a two-way ANOVA with Bonferroni correction was used to assess statistical differences between groups. Confidence intervals were set at 95%.

Results

Participants The *PRKAG3* R225W mutation carriers assessed in this study are a subset of the population

identified previously [18]. These participants were matched with control participants on the basis of sex, age, weight, BMI and physical activity. Physical activity was assessed through the International Physical Activity Questionnaire. No significant differences were noted in fasting values for plasma lipids, glucose, insulin and lactate in these individuals (Table 1).

Muscular fatigue R225W carriers demonstrated a remarkable resistance to fatigue relative to matched controls as assessed by electromyography during 60 s isometric contraction ($p<0.05$) (Fig. 1c). The rate of fatigue was determined by a linear regression of the mean frequency of contraction over time (mV/s). A negative slope (decrease in contraction frequency) is indicative of fatigue, whereas a flat line or positive slope indicates resistance to fatigue (representative electromyography traces) (Fig. 1a, b). Interestingly, the R225W carriers had an increase in mean frequency of contraction over time.

Fuel storage Previously our laboratory has shown ex vivo that muscle fibres from *PRKAG3* R225W carriers have ~30% lower IMTG content and ~90% higher glycogen content [18]. In the current study we examined fuel storage in satellite cells isolated from the vastus lateralis of R225W carriers. Myotubes from volunteers with the *PRKAG3* R225W mutation had ~30% more glycogen than myotubes from matched controls ($p<0.01$). Paradoxically, the acute treatment of control and R225W myotubes with AICAR resulted in a decrease in glycogen content ($p<0.001$) (Fig. 2a). Basal glycogen synthesis rates were 2.3-fold higher in R225W myotubes than in control myotubes (Fig. 2b). Insulin stimulation of the cells resulted in a 1.8-fold increase in glycogen synthesis rate in control myotubes, but had no effect on R225W myotubes ($p<0.05$) (Fig. 2b).

Myotubes from R225W carriers had somewhat decreased IMTG stores compared with cells from control participants (Fig. 2c). Interestingly, acute treatment of myotubes with the AMPK activator AICAR resulted in a trend towards decreased IMTG stores in the control cells, but not in the R225W cells.

Table 1 Baseline characteristics of carriers of the *PRKAG3* R225W mutation and matched controls

Characteristic	Control	R225W
Age (years)	44.3±5.2	43.5±7.7
BMI (kg/m^2)	28.6±4.1	29.6±4.2
Glucose (mmol/l)	4.83±0.22	4.95±0.38
Insulin (pmol/l)	0.085±0.011	0.108±0.019
Lactate (mmol/l)	1.47±0.014	1.60±0.014
Serum NEFA (mmol/l)	0.500±0.045	0.470±0.077
Maximal force output (N)	439.8±53.9	423.6±57.7

Values are means ± SEM

p=NS for all values, Student's t test

Fatty acid uptake and oxidation There were no differences in basal fatty acid uptake between control and R225W myotubes; however, control myotubes showed a ~20% increase in fatty acid uptake when stimulated with insulin, whereas R225W myotubes showed no change (Fig. 2d). Cells from R225W carriers exhibited a trend towards increased complete fatty acid oxidation, but this did not reach statistical significance. No differences were observed in incomplete fatty acid oxidation (Fig. 2e).

Oxidative capacity Mitochondrial content was threefold greater in myotubes from R225W carriers than in matched control participants ($p<0.01$) (Fig. 3a). Cytochrome *c* oxidase activity and citrate synthase activity were also measured as markers for electron transport chain and tricarboxylic acid (TCA) cycle capacity, respectively. R225W cells exhibited 2.5-fold higher cellular cytochrome *c* oxidase activity at the cellular level ($p<0.01$), but no difference in cytochrome *c* oxidase activity per mitochondrion (Fig. 3c, d). Interestingly, citrate synthase activity was ninefold higher in R225W myotubes at the cellular level ($p<0.05$) and threefold higher per mitochondrion ($p<0.05$), compared with control cells (Fig. 3e, f). These results are consistent with the idea that in R225W cells enhanced TCA cycle capacity is greater than that anticipated due to the increases in mitochondrial content. However, no significant differences were observed in the relative cellular amounts of the TCA cycle intermediates, succinate, α-ketoglutarate, citrate, fumarate or malate (ESM Methods and ESM Table 2).

We also tested for differences in oxidative characteristics of the cells by examining cellular oxygen consumption rates. Maximal oxygen consumption and mitochondrial proton leak-dependent respiration were evaluated in the presence of the chemical uncoupler FCCP or the inhibitor of ATP synthase, oligomycin. Myotubes from R225W carriers demonstrated ~2.5-fold higher maximal oxygen consumption ($p<0.01$) (Fig. 3b), consistent with the observed increases in mitochondrial content. They also exhibited elevated proton leak-dependent respiration ($p<0.05$) and a trend toward increased resting oxygen consumption. No significant differences were observed in extracellular acidification rate, a proxy measure of the rate of glycolysis (data not shown).

Gene expression and protein levels To assess factors mediating the increased mitochondrial content observed in R225W myotubes, mRNA expression levels of the mito-

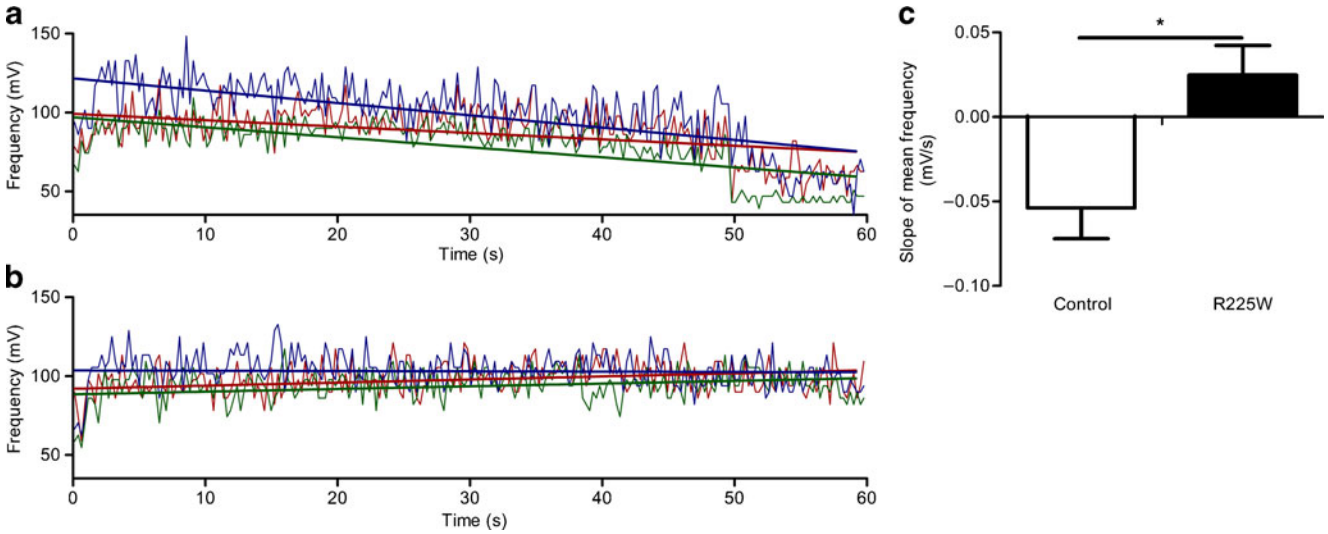

Fig. 1 Quadriceps maximal force and rate of fatigue. **a** Representative electromyography traces of the vastus lateralis (red), rectus femoris (green) and vastus medialis (blue) during the 60 s isometric contraction in control and **b** R225W carrier individuals. **c** Rates of fatigue as quantified by change in mean frequency of an isometric contraction at 80% of maximal concentric force over 60 s. Means ± SEM, n=4. *p<0.05 Student's t test

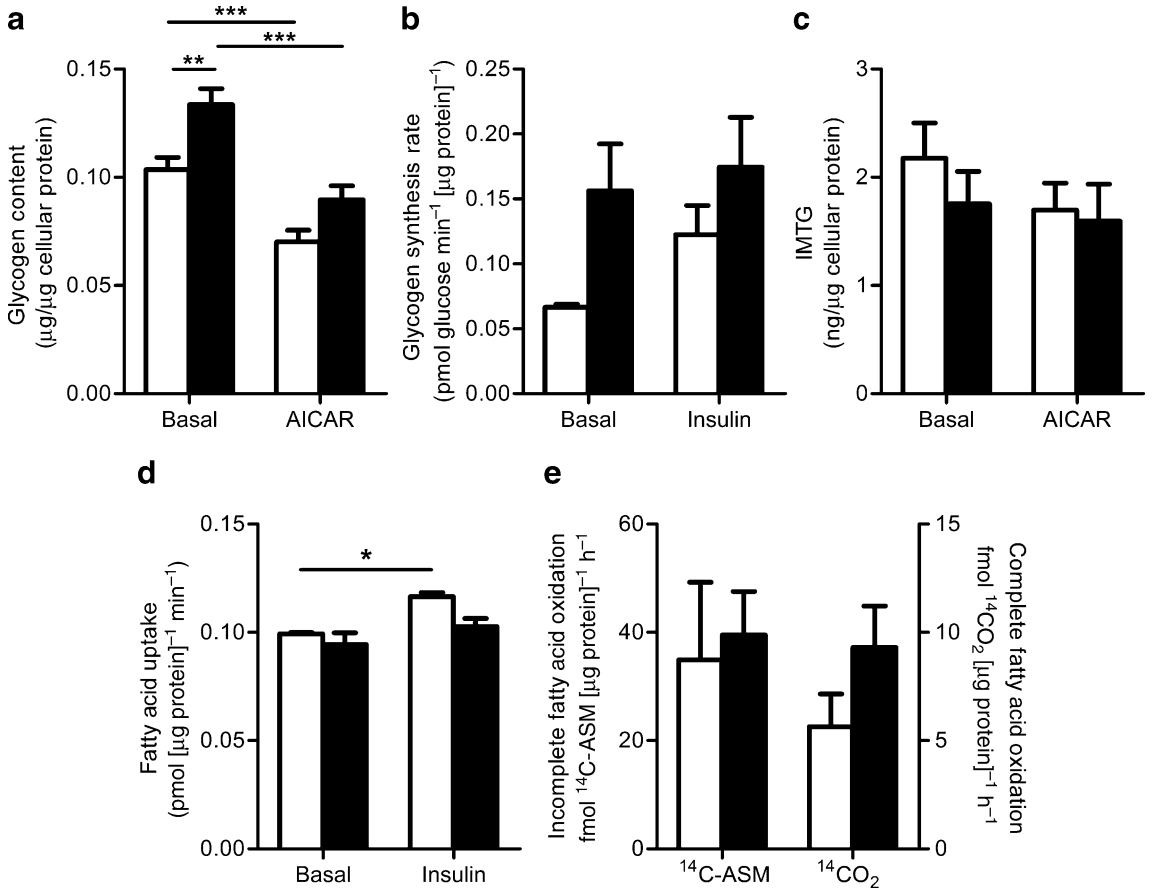

Fig. 2 Fuel storage in differentiated human myotubes. **a** Glycogen and **c** IMTG content normalised to total cellular protein in the basal state or following a 2 h treatment with 2 mmol/l AICAR. **b** Rate of glycogen re-synthesis following 1.5 h glucose/serum starvation in the presence or absence of 100 nmol/l insulin. **d** Rate of fatty acid uptake in the presence or absence of 100 nmol/l insulin. **e** Rate of incomplete and complete fatty acid oxidation expressed, respectively, as the rate of labelled acid soluble metabolite (^{14}C-ASM) and rate of CO_2 production ($^{14}CO_2$). Black bars, R225W carriers; white bars, control participants. Means ± SEM, n=3. p<0.05 for effect of genotype and treatment; *p<0.05, **p<0.01, ***p<0.001 (two-way ANOVA with Bonferroni correction)

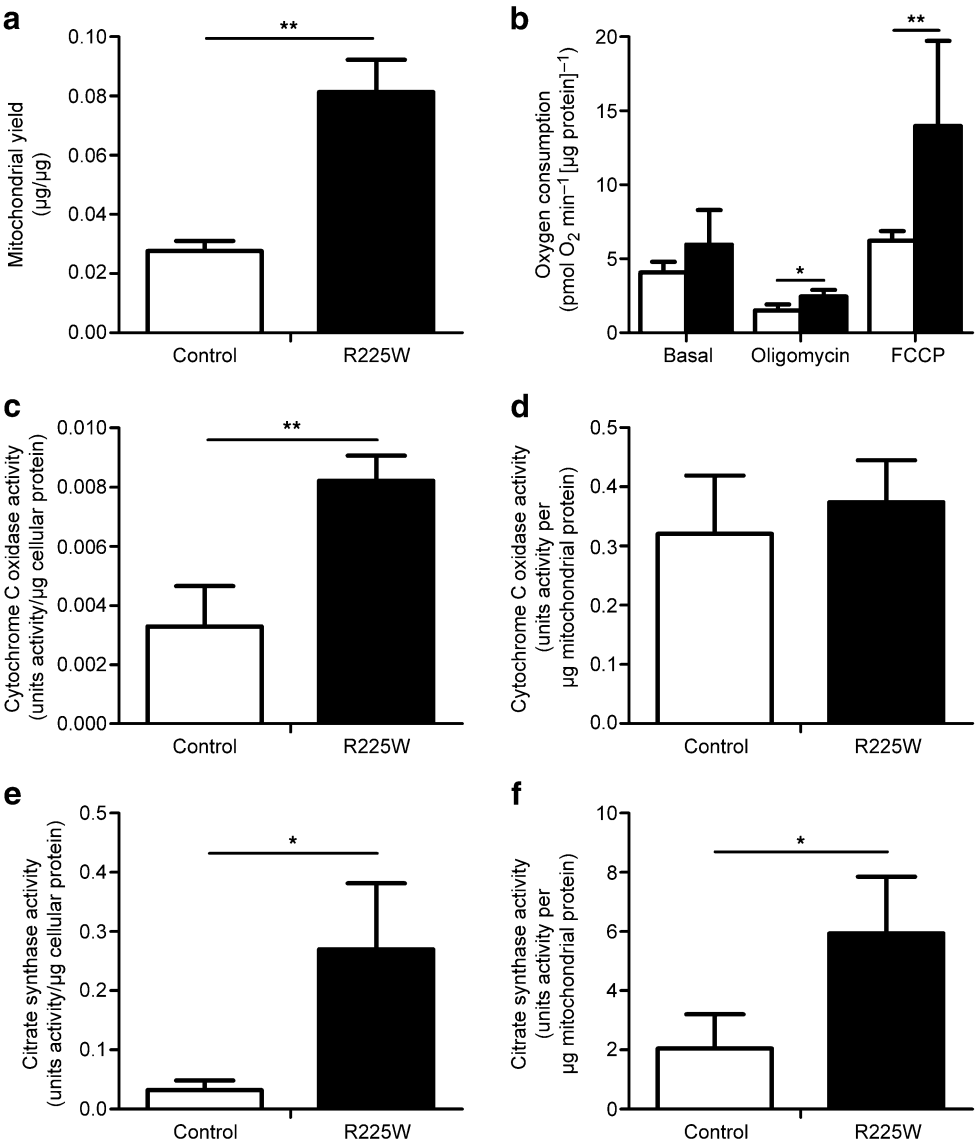

Fig. 3 Mitochondrial content and oxidative capacity in differentiated human myotubes. **a** Mitochondrial yield as mitochondrial protein content per cellular protein content. **b** Basal oxygen consumption, leak-dependent oxygen consumption (500 ng/ml oligomycin) and maximal oxygen consumption (1 μmol/l FCCP). Black bars, R225W carriers; white bars, control participants. **c** Cytochrome *c* oxidase activity normalised to cellular or **d** mitochondrial protein. **e** Citrate synthase activity normalised to cellular or **f** mitochondrial protein. Mean ± SEM, $n=3$. *$p<0.05$ and **$p<0.01$ (Student's *t* test)

chondrial transcription factors *PGC-1α*, *mTFA* and *NRF1* were quantified. While a trend for increased *PGC-1α* mRNA was observed, the inter-participant variability in these genes was much greater than any clear difference between groups (Fig. 4a). Protein levels of cytochrome *c* oxidase were found to be ~2.5-fold higher in R225W myotubes ($p<0.05$; Fig. 4b, c). The P-Akt:Akt ratio was moderately increased in R225W participants under basal conditions, but did not reach significance. There were no differences in P-Akt:Akt ratio between affected and control cells; however, the expected increases in phosphorylation upon addition of insulin were observed for both groups (Fig. 4b, d). No significant differences were observed in the protein levels of the transcription factor PGC1-α or the mitochondrial reactive oxygen species scavenger MnSOD (Fig. 4b, c).

Glucose uptake in vitro and in vivo Relative to control cells, R225W myotubes exhibited 80% higher basal glucose uptake rates ($p<0.01$) (Fig. 5a). R225W myotubes demonstrated similar absolute changes in glucose uptake following insulin stimulation relative to control myotubes (Fig. 5b).

Glucose uptake was measured in vivo by FDG-PET in resting and exercised quadriceps following a 30 min unilateral leg extension exercise against a constant resistance equivalent to 11% of the participant's maximal force output (Table 1). While three of the four R225W participants exhibited a trend towards increased total and maximal FDG uptake in the exercised leg ($p=0.054$), one exhibited very low levels of FDG uptake in the exercised leg (Fig. 6e, f). This latter individual also had elevated plasma cortisol outside the normal range (Fig. 6g). A larger volume of quadriceps muscle actively taking up FDG in the exercising leg was also apparent in R225W carriers, as defined by the volume of skeletal muscle meeting the threshold SUV of 1.0 in the exercising leg ($p<0.05$) (Fig. 6e). No differences were observed in the resting leg (data not shown). No differences

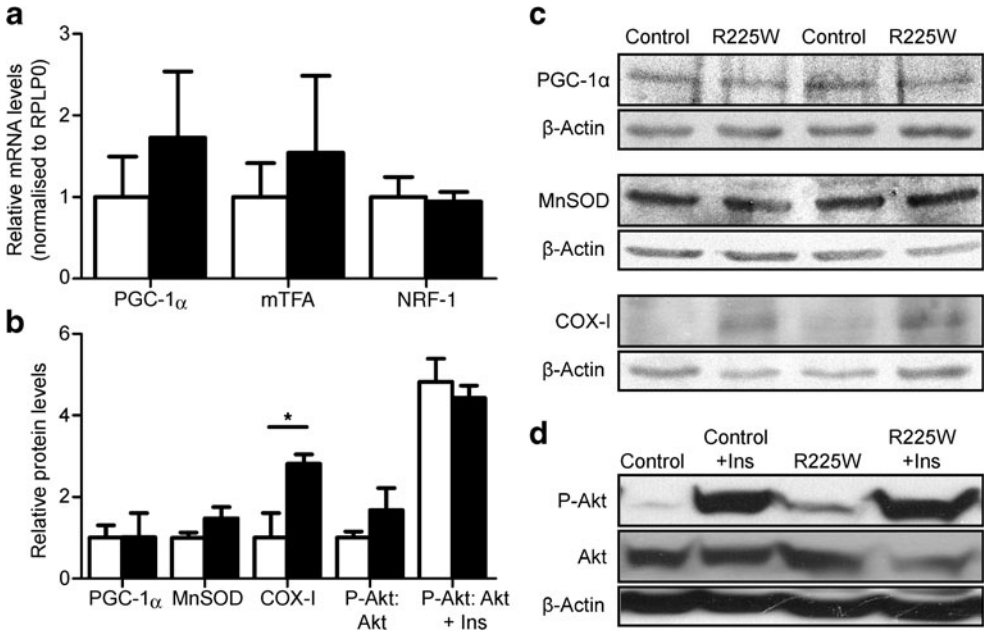

Fig. 4 mRNA expression and protein levels in differentiated human myotubes. **a** *PGC-1α*, *mTFA* and *NRF1* mRNA expression levels relative to *RPLP0*. **b** PGC-1α, MnSOD, cytochrome *c* oxidase (COX-I) and P-Akt protein levels relative to β-actin. P-Akt was produced in the presence and absence of 100 nmol/l insulin (Ins). Black bars, R225W carriers; white bars, control participants. **c**, **d** Representative western blots as labelled. Means ± SEM, $n=3$; *$p<0.05$ (Student's *t* test)

were observed in serum glucose or lactate with exercise; however, the relative increase in serum NEFA was higher in the carriers of the R225W mutation than in matched controls ($p<0.05$) (Table 2).

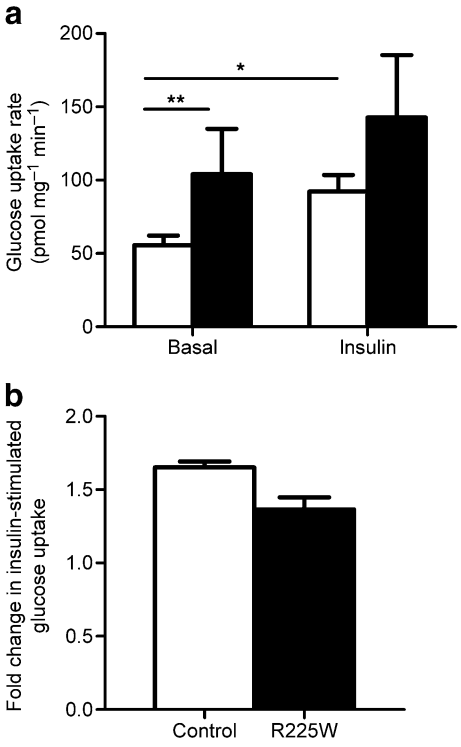

Fig. 5 Rate of glucose uptake in differentiated human myotubes. **a** Rate of glucose uptake in the presence or absence of 100 nmol/l insulin. **b** Fold-change in rate of glucose uptake following 100 nmol/l insulin stimulation. Black bars, R225W carriers; white bars, control participants. Means ± SEM, $n=3$; *$p<0.05$ and **$p<0.01$ (two-way ANOVA with Bonferroni correction)

Discussion

AMPK is an important regulator of cellular and whole-body energy metabolism. Despite extensive characterisation of acute AMPK activation, the metabolic effects of chronic AMPK activation, especially in humans, are poorly understood. In previous ex vivo histological analyses, we have shown that carriers of the *PRKAG3* R225W mutation have a 90% increase in skeletal muscle glycogen and a 30% decrease in IMTG stores compared with matched controls [18]. The current study further characterises the skeletal muscle metabolism of these participants in vivo and in vitro.

Consistent with AMPK's reported role in mitochondrial biogenesis through the induction of PGC-1α [11, 24], mitochondrial content and oxidative capacity were found to be significantly higher in the myotubes of R225W carriers than in myotubes of matched control participants. A trend for increased *PGC-1α* mRNA was observed in myotubes of R225W carriers, but there were no differences in PGC-1α protein levels. Despite the lack of change in protein levels, chronic AMPK activation may still result in indirect activation of PGC-1α. Jager et al. have previously shown that AMPK activation results in the phosphorylation of PGC-1α [11] and Canto et al. demonstrated that activation of AMPK results in activation of the NAD^+ dependent deacetylase, sirtuin 1, which in turn deacetylates and activates PGC-1α [41]. Mitochondrial leak-dependent respiration was also 1.6-fold higher in R225W myotubes, probably as a result of the increased mitochondrial content.

Interestingly, the activity of citrate synthase per mitochondrion was increased in R225W myotubes, suggesting enhanced TCA cycle capacity. Elevated glucose uptake in

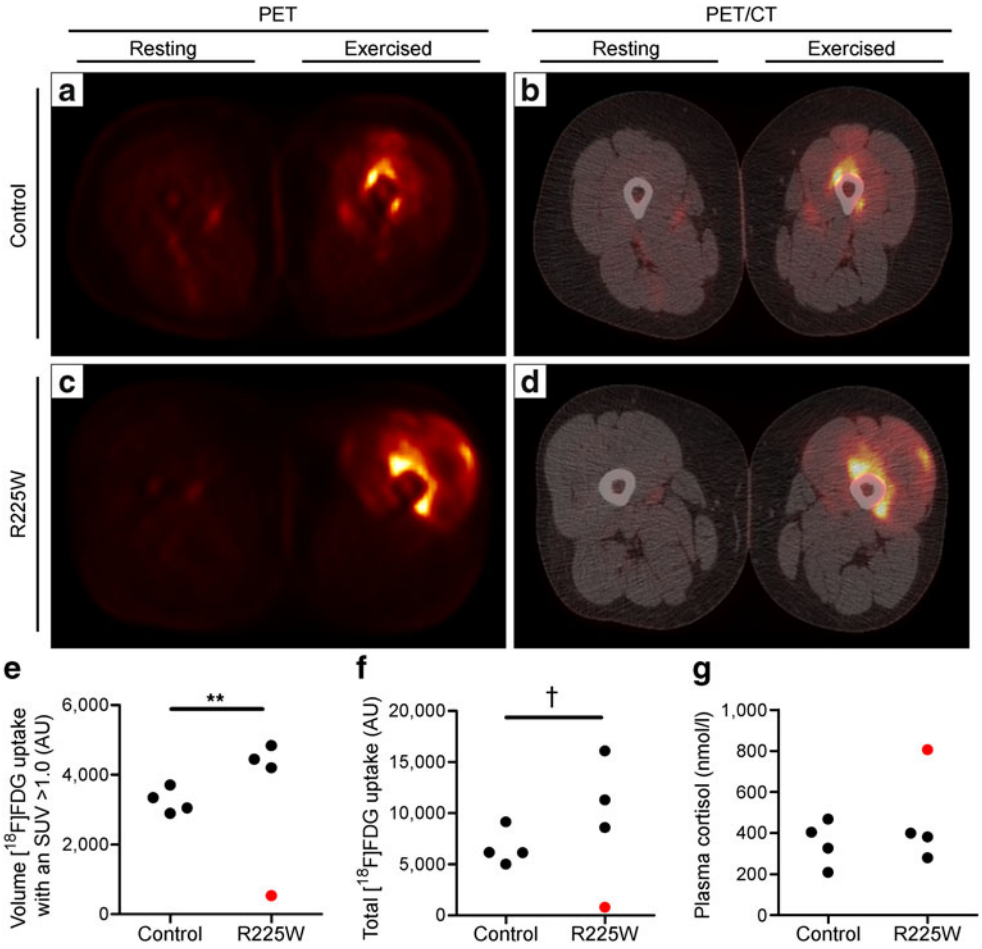

Fig. 6 Quadriceps glucose uptake in vivo. Participants performed a 30 min unilateral leg extension exercise with their dominant leg against a resistance equivalent to 11% of their maximal concentric force, followed by a PET/computed tomography (CT) scan. **a**, **c** Representative PET and **b**, **d** PET/computed tomography overlay images. **e** Total volume of muscle actively taking up glucose (SUV>1). **f** Total FDG uptake in the exercised leg. **g** Baseline plasma cortisol levels. Red symbols, outliers. $^{**}p<0.01$ and $^{\dagger}p=0.052$ (Student's *t* test)

myotubes of R225W participants may be responsible for the increases in TCA cycle activity (or vice versa); however, we were unable to detect differences in TCA metabolite levels. The lack of a corresponding increase in electron transport chain capacity (as measured by cytochrome *c* oxidase activity) suggests that these TCA cycle metabolites may be being diverted to alternative pathways.

R225W carriers also exhibited reduced rates of muscular fatigue, which is consistent with previous reports of increases in the time to 50% fatigue in mice with the analogous *Prkag3* R225Q mutation [42]. Based on results from the in vitro analyses, it is possible that the increase in isometric performance and resistance to fatigue in vivo is due to a combination of the increased glycogen content, glycogen synthesis rate and oxidative capacity seen in myotubes from carriers of the *PRKAG3* R225W mutation.

Table 2 Absolute changes in metabolites following a 30 min unilateral leg extension exercise against a resistance equivalent to 11% of maximal concentric force

Variable	Control	R225W	*p* value
Glucose (mmol/l)	0.040±0.065	0.060±0.078	NS
Insulin (pmol/l)	−0.003±0.014	0.030±0.027	NS
Lactate (mmol/l)	0.200±0.284	0.120±0.136	NS
Serum NEFA (mmol/l)	0.010±0.028	0.136±0.023	<0.05
Cortisol (nmol/l)	−35.32±29.80	−59.87±22.57	NS

Values are mean ± SEM

While previous studies have documented enhanced glucose uptake in response to acute activation of AMPK, either through exercise or treatment with AICAR in animal and cell culture models, respectively [28, 43], these effects have not been previously evaluated in humans in vivo. We examined the effects of the R225W mutation of the gene encoding AMPKγ3 on in vivo glucose uptake in exercised quadriceps as measured by FDG uptake using PET imaging. Three of four participants carrying the R225W polymorphism exhibited a larger volume of muscle actively taking up FDG as well as a trend towards increased total FDG uptake in the exercised quadriceps. The remaining carrier of the *PRKAG3* R225W mutation exhibited extremely low levels of FDG uptake. This low level of FDG uptake may be due, in part, to abnormally elevated levels of serum cortisol, a potent inhibitor of skeletal muscle glucose uptake [44]. This participant was not an outlier in any of the in vitro assays or in the muscular fatigue evaluations, suggesting that the increase in cortisol was likely to have

been a stress-related response to the testing protocol. The increase in plasma fatty acids in R225W carriers during exercise may indicate a blunted increase in fatty acid uptake in muscle in response to exercise, stemming in turn from a greater proportional reliance on endogenous glucose and glycogen fuel stores in the muscle of individuals with the *PRKAG3* R225W mutation.

The mechanism responsible for a greater glucose uptake in R225W carriers during exercise may be elevated skeletal muscle GLUT4 levels, which has been previously demonstrated in Sprague–Dawley rats chronically treated with AICAR [32]. However, *GLUT4* (also known as *SLC2A4*) expression in the control and R225W primary human myotubes was undetectable via quantitative RT-PCR (data not shown). Despite the very low *GLUT4* mRNA expression in human myotubes, rates of glucose uptake and glycogen synthesis in myotubes from R225W carriers were twofold higher than in matched controls. Moreover, there were no differences in insulin sensitivity. These results suggest that AMPK-mediated glucose uptake may be occurring through an insulin-independent pathway. Future studies are necessary to determine the mechanism by which glucose uptake in R225W myotubes is increased.

Despite the accepted role of AMPK in the inhibition of anabolic pathways such as glycogen synthesis, carriers of the *PRKAG3* R225W mutation have increased muscular glycogen stores [18]. This increase in basal glycogen storage is consistent with the increased rates of glycogen synthesis observed in the myotubes of affected individuals and the increased cardiomyocyte accumulation of glycogen observed in carriers of the homologous *PRKAG2* R302Q mutation [45]. During chronic AMPK activation, AMPK-stimulated glucose uptake may override inhibition of glycogen synthase by AMPK, resulting in enhanced glycogen storage. Similar effects of glycogen supercompensation have been previously observed in AICAR-treated Sprague–Dawley rats [32]. However, further AMPK activation through acute AICAR stimulation resulted in a decrease in glycogen levels in myotubes from control and R225W carriers. While this reduction in glycogen content following acute AICAR treatment may have resulted from the phosphorylation of glycogen synthase kinase by AMPK, it may also be the result of allosteric activation of glycogen phosphorylase by AICAR [26, 46, 47].

In vitro analysis of IMTG stores revealed a trend towards a slight decrease in R225W myotubes, which paralleled similar decreases in matched control participants following acute AMPK activation with AICAR. This trend is consistent with previous ex vivo histological analyses of these participants [18]. This modest decrease in IMTG content may be explained in part by a trend towards increased complete fatty acid oxidation in R225W myotubes. Acute activation of AMPK has been shown to result in the phosphorylation and inactivation of acetyl-CoA carboxylase, a key enzyme regulating the balance between fatty acid biosynthesis and oxidation [13, 48]. Inactivation of acetyl-CoA carboxylase leads to a decrease in fatty acid synthesis and a concomitant increase in fatty acid oxidation, resulting in depletion of IMTG stores [49, 50].

The observed decrease in IMTG content, and increases in glycogen content and oxidative capacity in human myotubes with the *PRKAG3* R225W mutation are consistent with the previous animal models with the homologous R225Q mutation [19, 23]. Interestingly, Barnes et al. have demonstrated that when fed a high-fat diet, mice expressing the *Prkag3* R225Q mutation were protected from skeletal muscle IMTG accumulation and insulin resistance relative to control and γ_3-knockout mice [23]. Similar studies in long-term AICAR treatment of rats reported reduced metabolic disturbances and lowered blood pressure in rats displaying features of the insulin resistance syndrome [51]. Finally, muscle-specific ablation of AMPKα_2 activity has been shown to exacerbate insulin resistance induced by high-fat feeding of mice [52].

In summary, the above findings of enhanced glucose uptake, oxidative capacity and delayed onset of muscular fatigue suggests that the *PRKAG3* R225W mutation may be beneficial to the exercise performance capabilities of affected participants. As a direct result of this mutation, these individuals are likely to have an enhanced capacity for endurance exercise. These results are also consistent with the hypothesis that the γ_3 subunit of AMPK may indeed be a suitable tissue-specific target for the treatment of type 2 diabetes mellitus, a condition in which glucose uptake and mitochondrial function are impaired.

Acknowledgements Financial support for this study was provided by the Heart and Stroke Foundation of Ontario (NA6200; to M. E. Harper and R. McPherson) and of Canada (PRG6242; to J. N. DaSilva, R. A. deKemp, R. S. B. Beanlands and M. E. Harper). The authors would like to thank L. Garrard for study coordination and M. Aung for assistance with PET analysis. We would also like to thank M. Lamontagne and E. Gannon for their contributions to the study design. Finally, we would like to thank S. Pagé for her assistance with isokinetic testing.

Duality of interest The authors declare that there is no duality of interest associated with this manuscript.

References

1. Hardie DG (2008) AMPK: a key regulator of energy balance in the single cell and the whole organism. Int J Obes (Lond) 32 (Suppl 4):S7–S12
2. Steinberg GR, Kemp BE (2009) AMPK in health and disease. Physiol Rev 89:1025–1078
3. Wojtaszewski JF, Birk JB, Frosig C, Holten M, Pilegaard H, Dela F (2005) 5'AMP activated protein kinase expression in human

skeletal muscle: effects of strength training and type 2 diabetes. J Physiol 564:563–573
4. Mahlapuu M, Johansson C, Lindgren K et al (2004) Expression profiling of the gamma-subunit isoforms of AMP-activated protein kinase suggests a major role for gamma3 in white skeletal muscle. Am J Physiol Endocrinol Metab 286:E194–E200
5. Yu H, Fujii N, Hirshman MF, Pomerleau JM, Goodyear LJ (2004) Cloning and characterization of mouse 5'-AMP-activated protein kinase gamma3 subunit. Am J Physiol Cell Physiol 286:C283–C292
6. Yeh LA, Lee KH, Kim KH (1980) Regulation of rat liver acetyl-CoA carboxylase. Regulation of phosphorylation and inactivation of acetyl-CoA carboxylase by the adenylate energy charge. J Biol Chem 255:2308–2314
7. Hawley SA, Boudeau J, Reid JL et al (2003) Complexes between the LKB1 tumor suppressor, STRAD alpha/beta and MO25 alpha/beta are upstream kinases in the AMP-activated protein kinase cascade. J Biol 2:28
8. Sakamoto K, McCarthy A, Smith D et al (2005) Deficiency of LKB1 in skeletal muscle prevents AMPK activation and glucose uptake during contraction. EMBO J 24:1810–1820
9. McBride A, Ghilagaber S, Nikolaev A, Hardie DG (2009) The glycogen-binding domain on the AMPK beta subunit allows the kinase to act as a glycogen sensor. Cell Metab 9:23–34
10. Suwa M, Nakano H, Kumagai S (2003) Effects of chronic AICAR treatment on fiber composition, enzyme activity, UCP3, and PGC-1 in rat muscles. J Appl Physiol 95:960–968
11. Jager S, Handschin C, St-Pierre J, Spiegelman BM (2007) AMP-activated protein kinase (AMPK) action in skeletal muscle via direct phosphorylation of PGC-1alpha. Proc Natl Acad Sci U S A 104:12017–12022
12. Koistinen HA, Galuska D, Chibalin AV et al (2003) 5-amino-imidazole carboxamide riboside increases glucose transport and cell-surface GLUT4 content in skeletal muscle from subjects with type 2 diabetes. Diabetes 52:1066–1072
13. Corton JM, Gillespie JG, Hardie DG (1994) Role of the AMP-activated protein kinase in the cellular stress response. Curr Biol 4:315–324
14. Foretz M, Carling D, Guichard C, Ferre P, Foufelle F (1998) AMP-activated protein kinase inhibits the glucose-activated expression of fatty acid synthase gene in rat hepatocytes. J Biol Chem 273:14767–14771
15. Foretz M, Ancellin N, Andreelli F et al (2005) Short-term overexpression of a constitutively active form of AMP-activated protein kinase in the liver leads to mild hypoglycemia and fatty liver. Diabetes 54:1331–1339
16. Woods A, Azzout-Marniche D, Foretz M et al (2000) Characterization of the role of AMP-activated protein kinase in the regulation of glucose-activated gene expression using constitutively active and dominant negative forms of the kinase. Mol Cell Biol 20:6704–6711
17. Leclerc I, Kahn A, Doiron B (1998) The 5'-AMP-activated protein kinase inhibits the transcriptional stimulation by glucose in liver cells, acting through the glucose response complex. FEBS Lett 431:180–184
18. Costford SR, Kavaslar N, Ahituv N et al (2007) Gain-of-function R225W mutation in human AMPKgamma3 causing increased glycogen and decreased triglyceride in skeletal muscle. PLoS ONE 2:e903
19. Milan D, Jeon JT, Looft C et al (2000) A mutation in PRKAG3 associated with excess glycogen content in pig skeletal muscle. Science 288:1248–1251
20. Arad M, Benson DW, Perez-Atayde AR et al (2002) Constitutively active AMP kinase mutations cause glycogen storage disease mimicking hypertrophic cardiomyopathy. J Clin Invest 109:357–362
21. Gollob MH, Seger JJ, Gollob TN et al (2001) Novel PRKAG2 mutation responsible for the genetic syndrome of ventricular preexcitation and conduction system disease with childhood onset and absence of cardiac hypertrophy. Circulation 104:3030–3033
22. Gollob MH, Green MS, Tang AS et al (2001) Identification of a gene responsible for familial Wolff–Parkinson–White syndrome. N Engl J Med 344:1823–1831
23. Barnes BR, Marklund S, Steiler TL et al (2004) The 5'-AMP-activated protein kinase gamma3 isoform has a key role in carbohydrate and lipid metabolism in glycolytic skeletal muscle. J Biol Chem 279:38441–38447
24. Garcia-Roves PM, Osler ME, Holmstrom MH, Zierath JR (2008) Gain-of-function R225Q mutation in AMP-activated protein kinase gamma3 subunit increases mitochondrial biogenesis in glycolytic skeletal muscle. J Biol Chem 283:35724–35734
25. Carling D, Hardie DG (1989) The substrate and sequence specificity of the AMP-activated protein kinase. Phosphorylation of glycogen synthase and phosphorylase kinase. Biochim Biophys Acta 1012:81–86
26. Aschenbach WG, Hirshman MF, Fujii N, Sakamoto K, Howlett KF, Goodyear LJ (2002) Effect of AICAR treatment on glycogen metabolism in skeletal muscle. Diabetes 51:567–573
27. Russell RR 3rd, Bergeron R, Shulman GI, Young LH (1999) Translocation of myocardial GLUT-4 and increased glucose uptake through activation of AMPK by AICAR. Am J Physiol 277:H643–H649
28. Kurth-Kraczek EJ, Hirshman MF, Goodyear LJ, Winder WW (1999) 5' AMP-activated protein kinase activation causes GLUT4 translocation in skeletal muscle. Diabetes 48:1667–1671
29. Jorgensen SB, Viollet B, Andreelli F et al (2004) Knockout of the alpha2 but not alpha1 5'-AMP-activated protein kinase isoform abolishes 5-aminoimidazole-4-carboxamide-1-beta-4-ribofuranoside but not contraction-induced glucose uptake in skeletal muscle. J Biol Chem 279:1070–1079
30. Geraghty KM, Chen S, Harthill JE et al (2007) Regulation of multisite phosphorylation and 14-3-3 binding of AS160 in response to IGF-1, EGF, PMA and AICAR. Biochem J 407:231–241
31. Jakobsen SN, Hardie DG, Morrice N, Tornqvist HE (2001) 5'-AMP-activated protein kinase phosphorylates IRS-1 on Ser-789 in mouse C2C12 myotubes in response to 5-aminoimidazole-4-carboxamide riboside. J Biol Chem 276:46912–46916
32. Holmes BF, Kurth-Kraczek EJ, Winder WW (1999) Chronic activation of 5'-AMP-activated protein kinase increases GLUT-4, hexokinase, and glycogen in muscle. J Appl Physiol 87:1990–1995
33. Beanlands RTS, DaSilva J, Ruddy T, Maddahi J (2008) Myocardial viability. In: Wahl RL (ed) Principles and Practices of PET and PET/CT. Lippincott Williams and Wilkins, Philadelphia
34. Kemppainen J, Fujimoto T, Kalliokoski KK, Viljanen T, Nuutila P, Knuuti J (2002) Myocardial and skeletal muscle glucose uptake during exercise in humans. J Physiol 542:403–412
35. Kalliokoski KK, Langberg H, Ryberg AK et al (2005) The effect of dynamic knee-extension exercise on patellar tendon and quadriceps femoris muscle glucose uptake in humans studied by positron emission tomography. J Appl Physiol 99:1189–1192
36. Developmental Studies Hybridoma Bank. Available from http://dshb.biology.uiowa.edu/, accessed 1 January 2009
37. Kim JY, Hickner RC, Cortright RL, Dohm GL, Houmard JA (2000) Lipid oxidation is reduced in obese human skeletal muscle. Am J Physiol Endocrinol Metab 279:E1039–E1044
38. Pimenta AS, Gaidhu MP, Habib S et al (2008) Prolonged exposure to palmitate impairs fatty acid oxidation despite activation of AMP-activated protein kinase in skeletal muscle cells. J Cell Physiol 217:478–485

39. McIntyre EA, Halse R, Yeaman SJ, Walker M (2004) Cultured muscle cells from insulin-resistant type 2 diabetes patients have impaired insulin, but normal 5-amino-4-imidazolecarboxamide riboside-stimulated, glucose uptake. J Clin Endocrinol Metab 89:3440–3448
40. Wensaas AJ, Rustan AC, Lovstedt K et al (2007) Cell-based multiwell assays for the detection of substrate accumulation and oxidation. J Lipid Res 48:961–967
41. Canto C, Gerhart-Hines Z, Feige JN et al (2009) AMPK regulates energy expenditure by modulating NAD+ metabolism and SIRT1 activity. Nature 458:1056–1060
42. Barnes BR, Glund S, Long YC, Hjalm G, Andersson L, Zierath JR (2005) 5'-AMP-activated protein kinase regulates skeletal muscle glycogen content and ergogenics. FASEB J 19:773–779
43. Mu J, Brozinick JT Jr, Valladares O, Bucan M, Birnbaum MJ (2001) A role for AMP-activated protein kinase in contraction- and hypoxia-regulated glucose transport in skeletal muscle. Mol Cell 7:1085–1094
44. Curry DL, Bennett LL (1973) Dynamics of insulin release by perfused rat pancreases: effects of hypophysectomy, growth hormone, adrenocorticotropic hormone, and hydrocortisone. Endocrinology 93:602–609
45. Folmes KD, Chan AY, Koonen DP et al (2009) Distinct early signaling events resulting from the expression of the PRKAG2 R302Q mutant of AMPK contribute to increased myocardial glycogen. Circ Cardiovasc Genet 2:457–466
46. Longnus SL, Wambolt RB, Parsons HL, Brownsey RW, Allard MF (2003) 5-Aminoimidazole-4-carboxamide 1-beta-D-ribofuranoside (AICAR) stimulates myocardial glycogenolysis by allosteric mechanisms. Am J Physiol Regul Integr Comp Physiol 284:R936–R944
47. Horike N, Sakoda H, Kushiyama A et al (2008) AMP-activated protein kinase activation increases phosphorylation of glycogen synthase kinase 3beta and thereby reduces cAMP-responsive element transcriptional activity and phosphoenolpyruvate carboxykinase C gene expression in the liver. J Biol Chem 283:33902–33910
48. Henin N, Vincent MF, Gruber HE, Van den Berghe G (1995) Inhibition of fatty acid and cholesterol synthesis by stimulation of AMP-activated protein kinase. FASEB J 9:541–546
49. Velasco G, Geelen MJ, Guzman M (1997) Control of hepatic fatty acid oxidation by 5'-AMP-activated protein kinase involves a malonyl-CoA-dependent and a malonyl-CoA-independent mechanism. Arch Biochem Biophys 337:169–175
50. Brusq JM, Ancellin N, Grondin P et al (2006) Inhibition of lipid synthesis through activation of AMP kinase: an additional mechanism for the hypolipidemic effects of berberine. J Lipid Res 47:1281–1288
51. Buhl ES, Jessen N, Schmitz O et al (2001) Chronic treatment with 5-aminoimidazole-4-carboxamide-1-beta-D-ribofuranoside increases insulin-stimulated glucose uptake and GLUT4 translocation in rat skeletal muscles in a fiber type-specific manner. Diabetes 50:12–17
52. Fujii N, Ho RC, Manabe Y et al (2008) Ablation of AMP-activated protein kinase alpha2 activity exacerbates insulin resistance induced by high-fat feeding of mice. Diabetes 57:2958–2966